

Supporting Information of

Semimetallic Carbon Honeycombs: New Three-dimensional Graphene Allotropes with Dirac Cones

Shuaiwei Wang^{ab}, Donghai Wu^{ab}, Baocheng Yang^{ab}, Eli Ruckenstein^c, Houyang Chen^{c*}

^aInstitute of Nanostructured Functional Materials, Huanghe Science and Technology College,

Zhengzhou, Henan 450006, China

^bHenan provincial key laboratory of nano-composite and applications, Zhengzhou, Henan 450006,

China

^cDepartment of Chemical and Biological Engineering, State University of New York at Buffalo,

Buffalo, New York 14260-4200, USA

* To whom correspondence should be addressed. Email: hchen23@buffalo.edu

Section S1. Computational methods

Vienna *ab initio* simulation package (VASP)^{1, 2} is employed to perform the DFT calculations. The ion-electron interactions were described by projector-augmented plane wave (PAW)³ potential. The electron exchange-correlation energy was treated by the generalized gradient approximation (GGA) with Perdew-Burle-Ernzerhof (PBE) functional⁴. The energy cutoff of plane waves was set to 600 eV and the energy convergence criterion between two steps was set at 10^{-8} eV. The atomic structures were fully relaxed using the conjugate gradients (CG) method until the maximum force on each atom was less than 10^{-2} eV \AA^{-1} . The Brillouin zone (BZ) was sampled with a spacing of $2\pi \times 0.00667 \text{\AA}^{-1}$ for self-consistent calculations and of $2\pi \times 0.02 \text{\AA}^{-1}$ for geometry optimization, band structures, density of states, and charge density.

The phonon dispersion analysis was performed by using the Phonopy⁵. The *ab initio* molecular dynamics (AIMD) simulations were carried out to evaluate the thermal stability of all newly designed CHC structures. AIMD simulation under constant temperature and volume (NVT) ensemble lasts for 5 ps with a time step of 1.0 fs. The temperature was controlled by using the Nosé-Hoover method⁶.

The atomic positions can be fully relaxed under the condition of tensile or compressive strain. The lattice constants are fixed in the tensile or compressive strain direction, while the other directions can relax.

Table S1. **Elastic constants** C_{ij} (GPa) of *Cmcm*-CHC-1, *Cmmm*-CHC-1, *Cmcm*-CHC-2, *Cmmm*-CHC-2, Graphene, and Diamond.

	<i>Cmcm</i> -		<i>Cmmm</i> -		Graphene	Diamond
	CHC-1	CHC-2	CHC-1	CHC-2		
C_{11}	507	253	318	208	1053 ^a	1049 ^b
C_{22}	378	132	213	91	1053 ^a	
C_{33}	1203	541	740	426		
C_{12}	242	97	137	76	178 ^a	124 ^b
C_{13}	69	39	46	35		
C_{23}	55	27	36	24		
C_{44}	266	94	140	70		
C_{55}	298	141	182	116		
C_{66}	306	104	149	80		561 ^b

^a DFT calculations in Ref.⁷

^b DFT calculations in Ref.⁸

^c Ref.⁹

Figure S1. The geometries of 3D carbon honeycomb (CHC) networks: (a) *Pmm2*-CHC-1, (b) *Pmmm*-CHC-1, (c) *Pmma*-CHC-1, and (d) *Amm2*-CHC-1

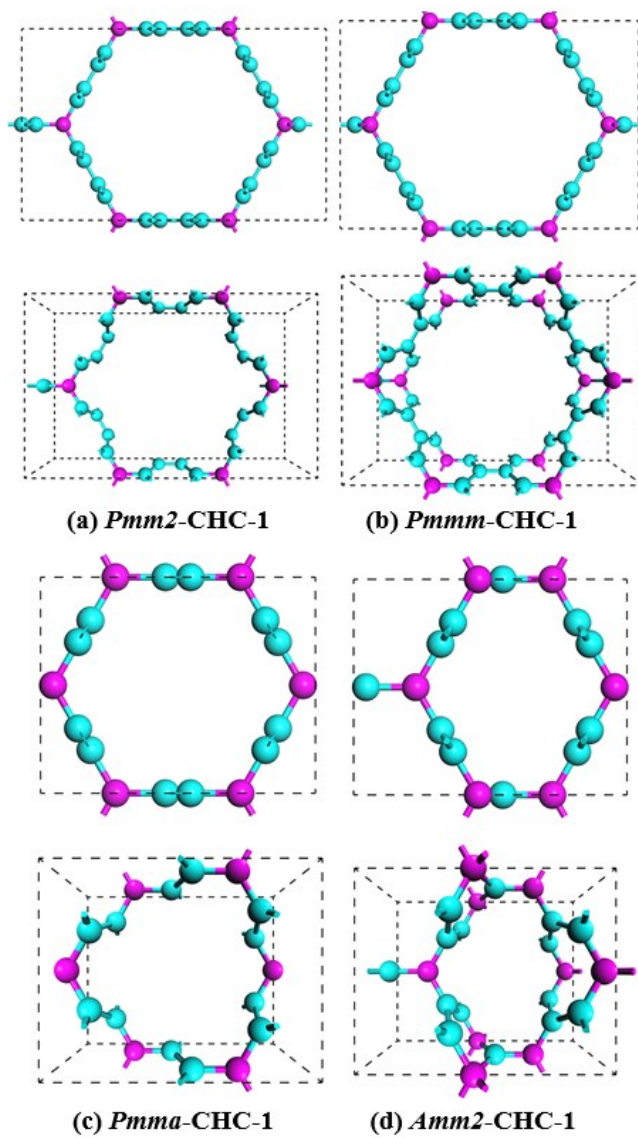


Figure S2. **Phonon dispersion** of *Cmcm*-CHC-1 (a), *Cmcm*-CHC-2 (b), *Cmmm*-CHC-1 (c) and *Cmmm*-CHC-2 (d).

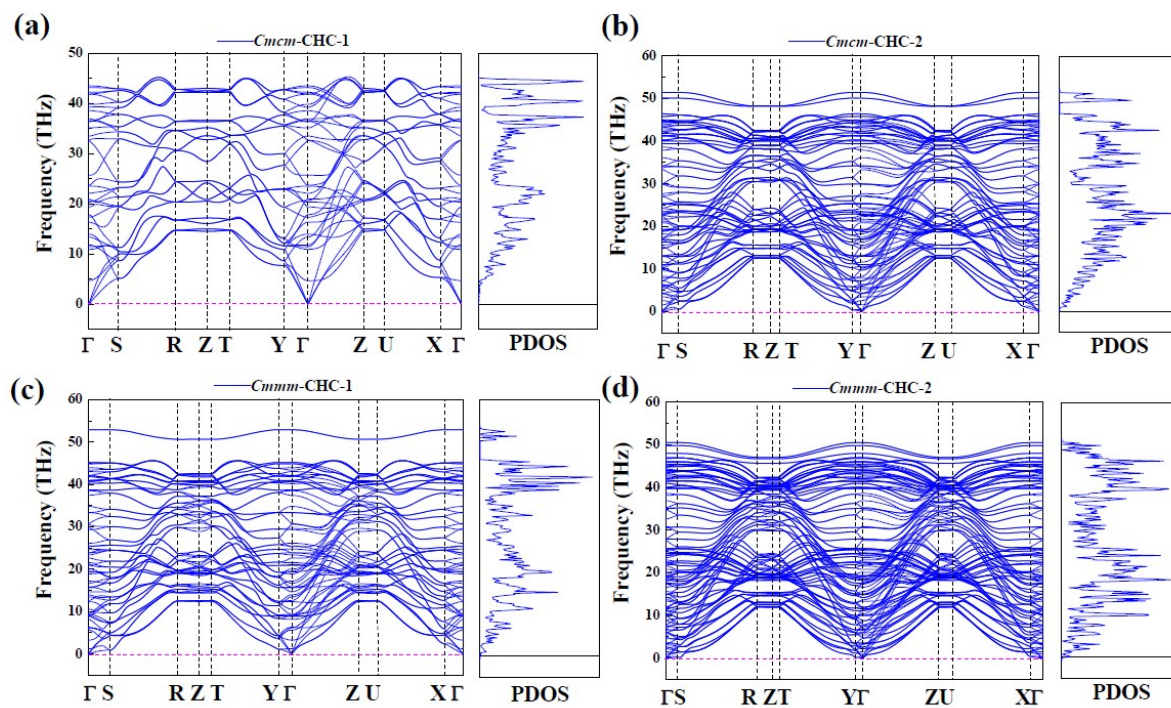


Figure S3. Phonon dispersion of 3D carbon honeycomb networks: (a) $Pmm2$ -CHC-1, (b) $Pmmm$ -CHC-1, (c) $Pmma$ -CHC-1, and (d) $Amm2$ -CHC-1

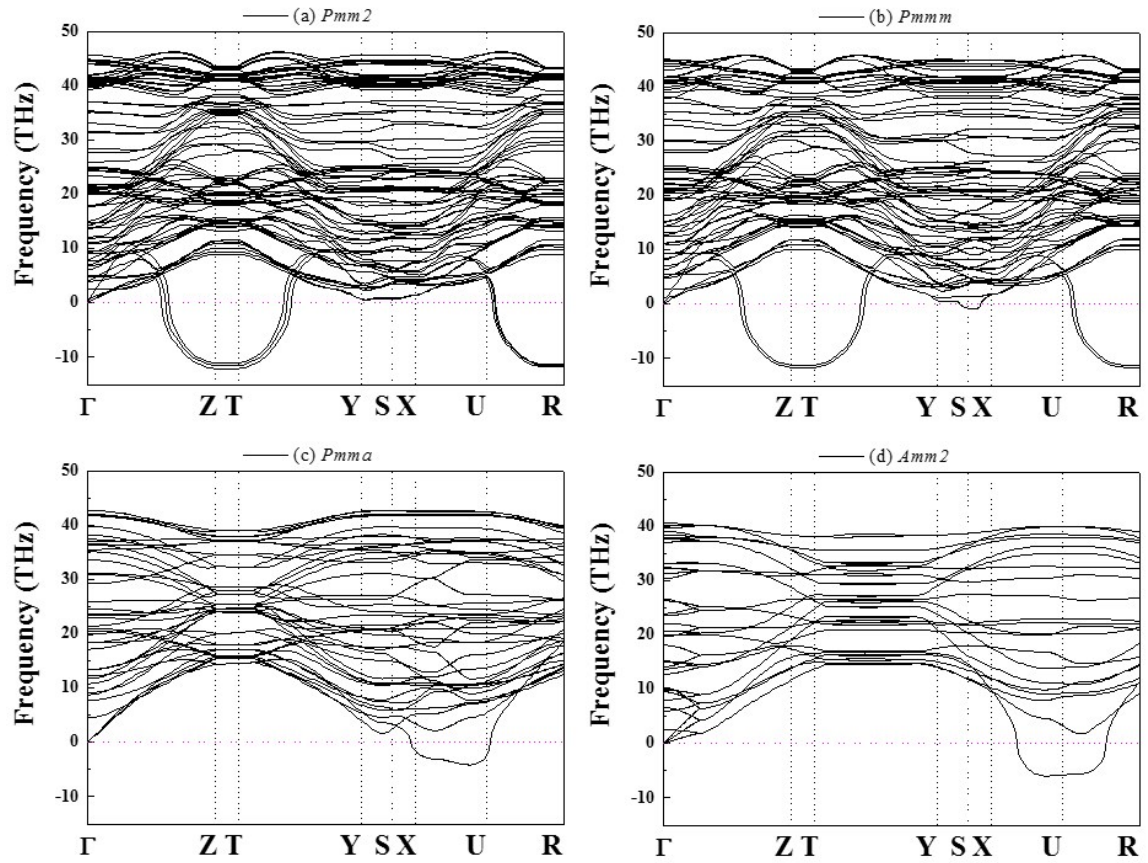


Figure S4. **Thermal stability.** The snapshots of (a-c) *Cmcm*-CHC-1 and (d-f) *Cmmm*-CHC-1 at (a,d) 300 K, (b,e) 1000 K, and (c,f) 1500 K at the end of 5 fs, and the fluctuations of total potential energy as functions of time for *Cmcm*-CHC-1 (g) and *Cmmm*-CHC-1 (h).

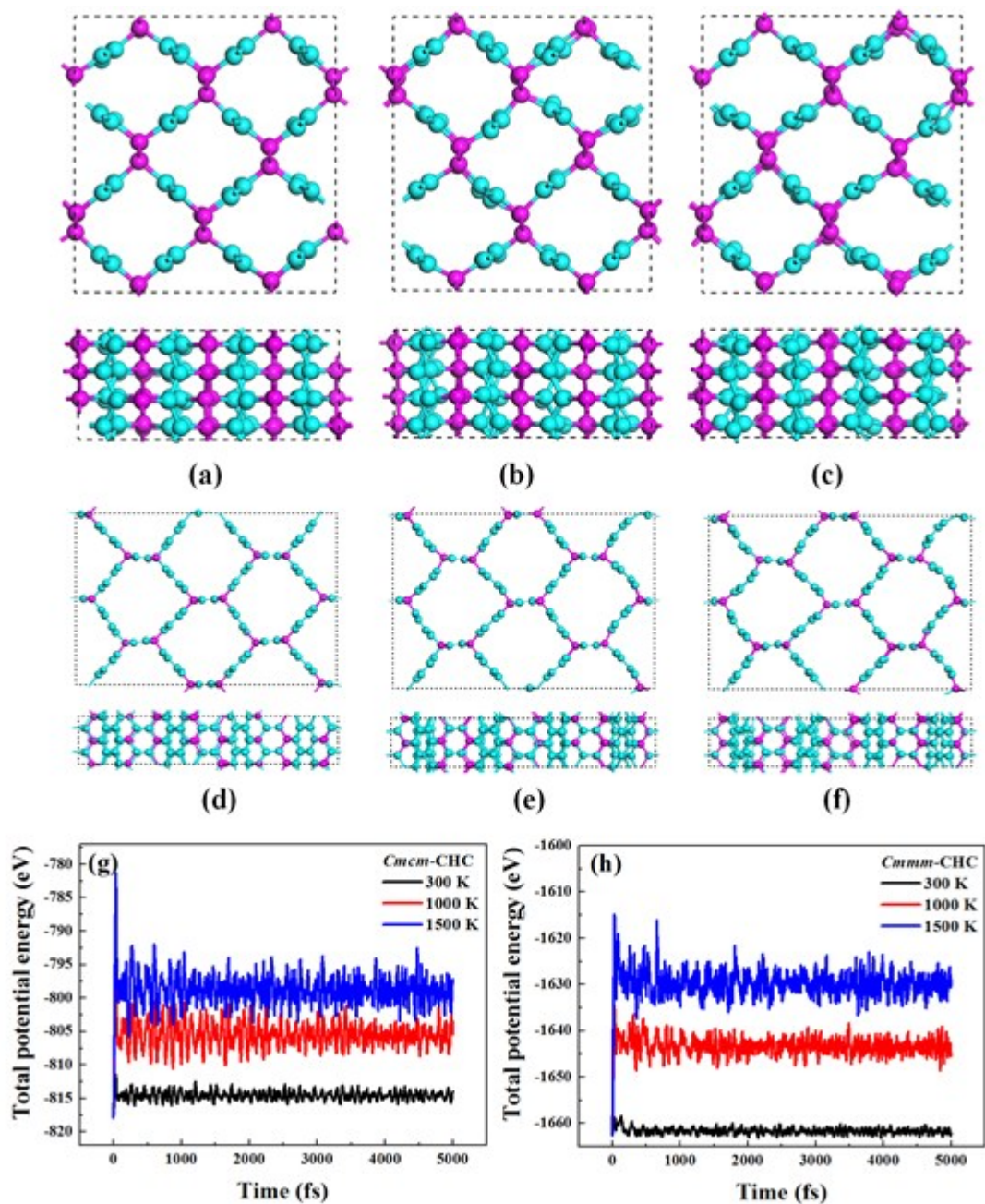


Figure S5. **Band structures and projected DOS.** (a) *Cmcm*-CHC-2, (b) *Cmmm*-CHC-2, (c) *Cmcm*-CHC-3, and (d) *Cmmm*-CHC-3.

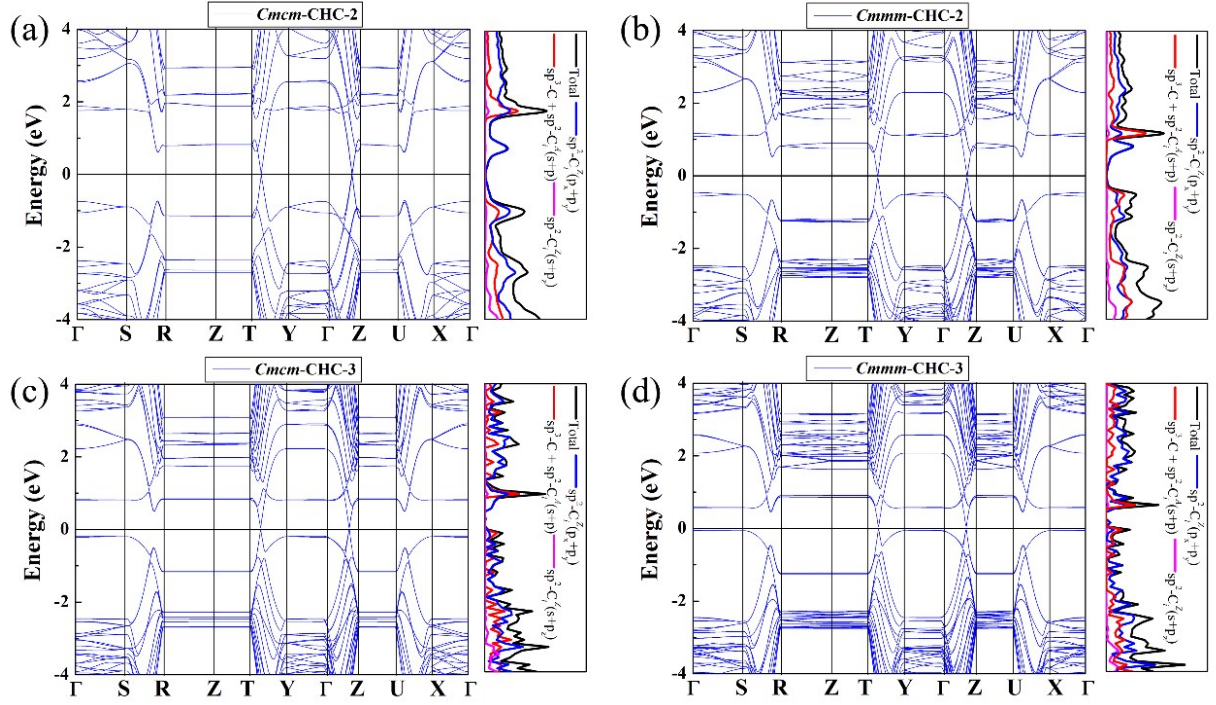


Figure S6. **Tight binding parameters.** The hopping energy parameters of *Cmcm*-CHC-1 (a) and *Cmmm*-CHC-1 (b) at the strain of -15% along the armchair direction.

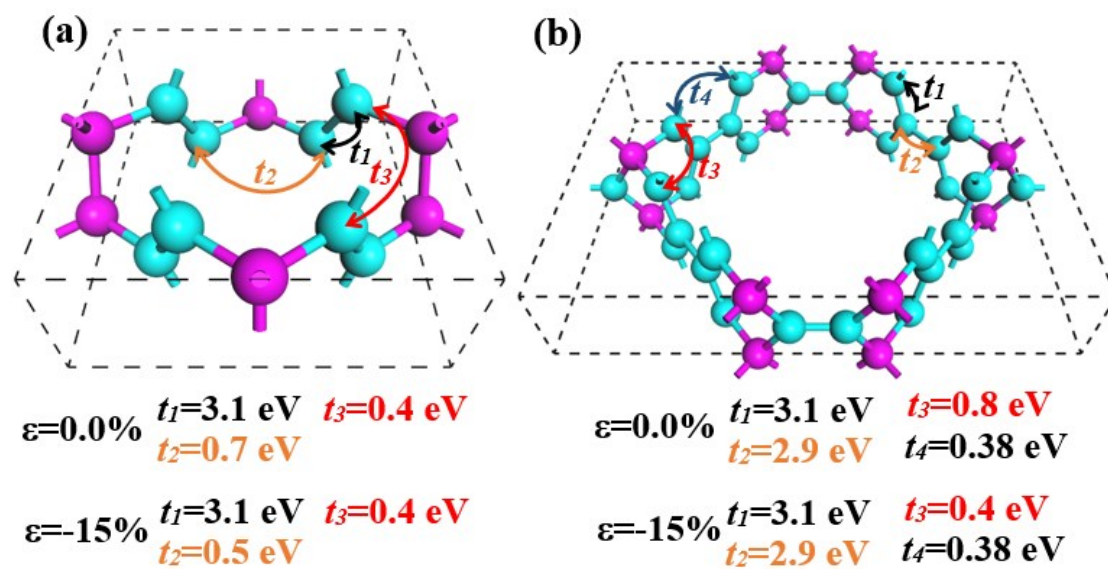


Figure S7. Band structures with SOC of *Cmcm*-CHC-1 (a) and *Cmmm*-CHC-1 (b).

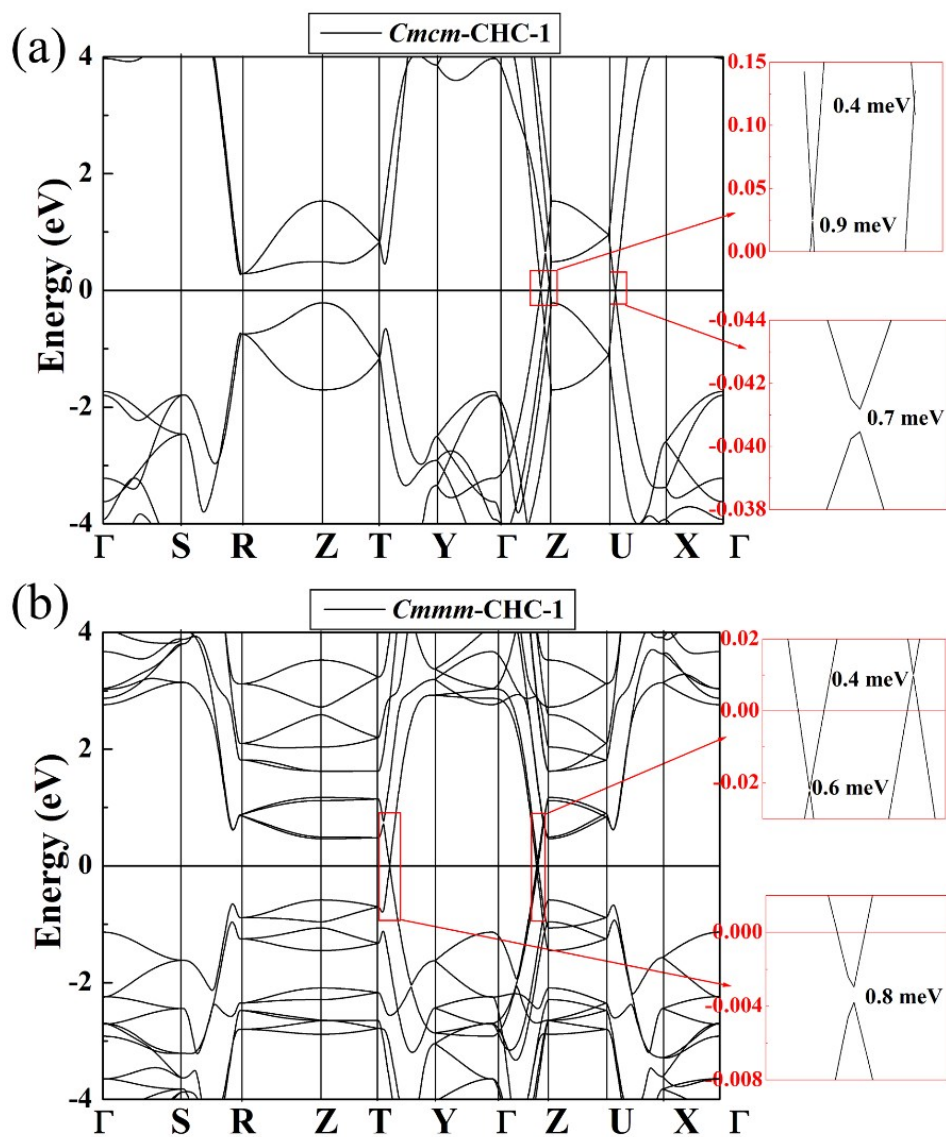


Figure S8. **Band structures** along Γ -Z and X-U lines of *Cmcm*-CHC-1 at strain $\pm 5\%$

along x , y , and z axis, respectively. Fermi level has been set to zero.

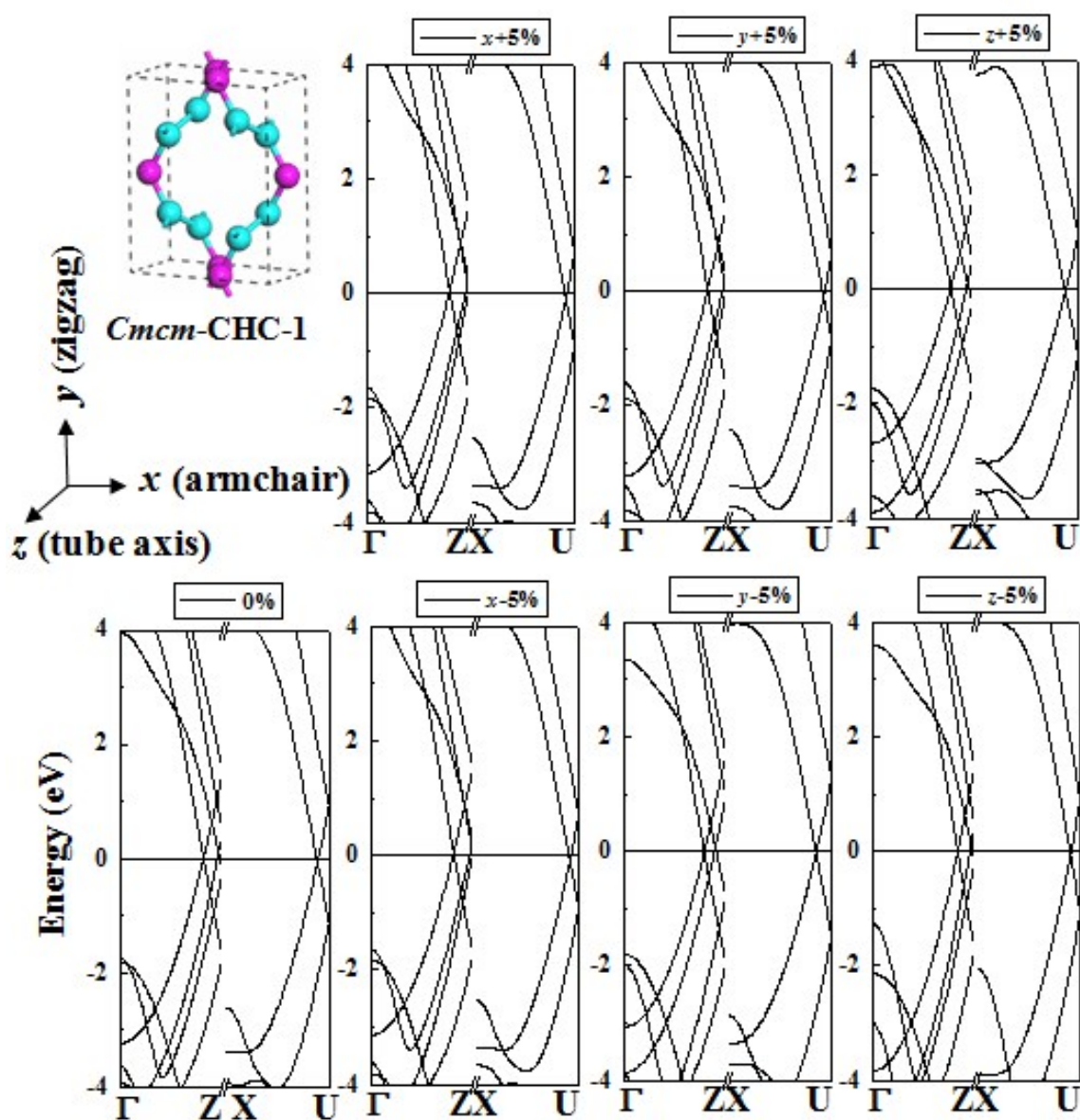


Figure S9. **Band structures** along Γ -Z and X-U lines of *Cmmm*-CHC-1 at strain

$\pm 5\%$ along x , y , and z axis, respectively. Fermi level has been set to zero.

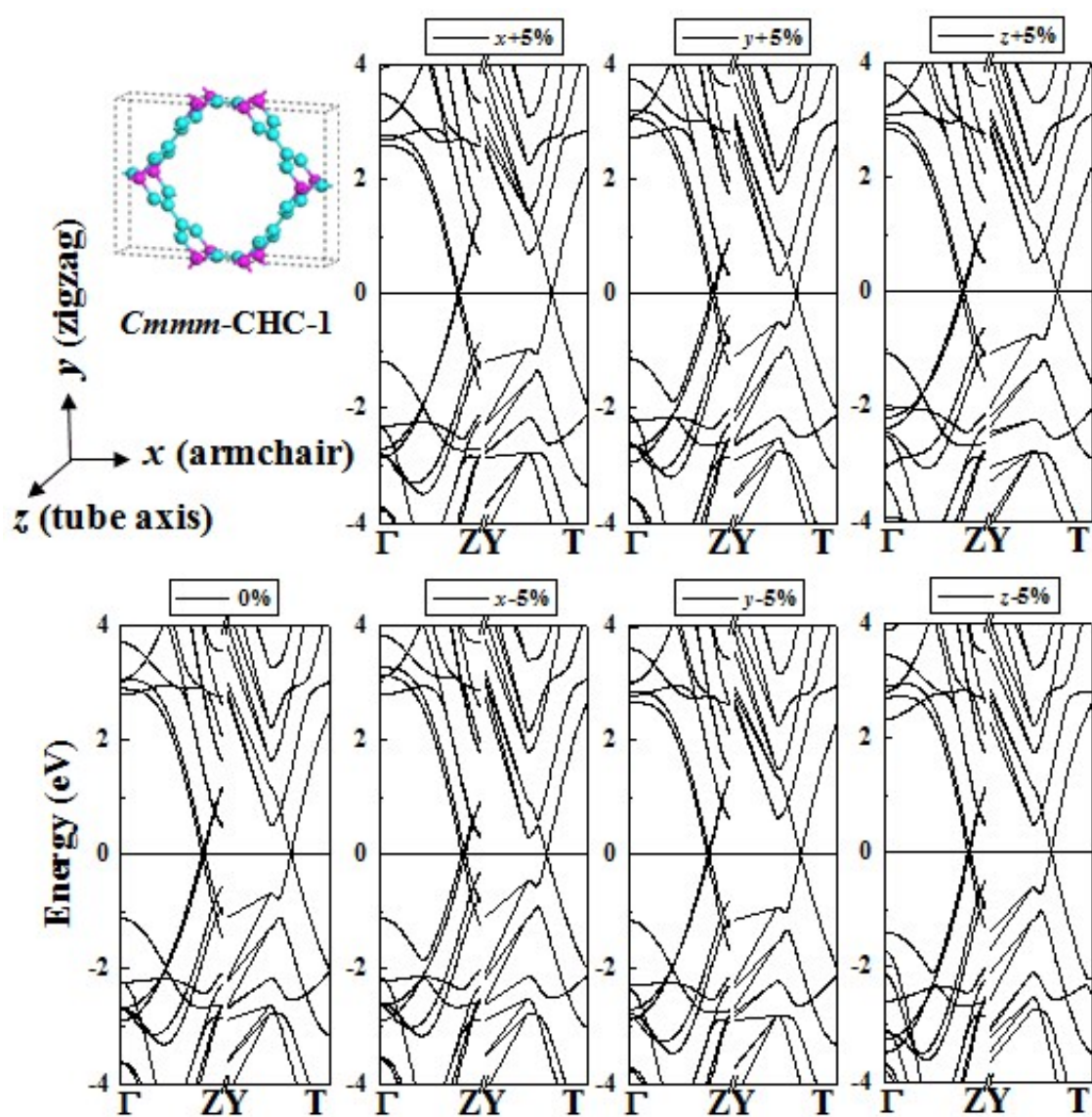


Figure S10. **Phonon dispersion.** (a) *Cmcm*-CHC-1 and (b) *Cmmm*-CHC-1 at the strain of -15% (compression), (c) *Cmmm*-CHC-1 at the strain of -35% (compression), (d) *Cmmm*-CHC-1 at the strain of -36% (compression) along the armchair direction, and (e) the structure of *Cmmm*-CHC-1 at strain of -35% (compression).

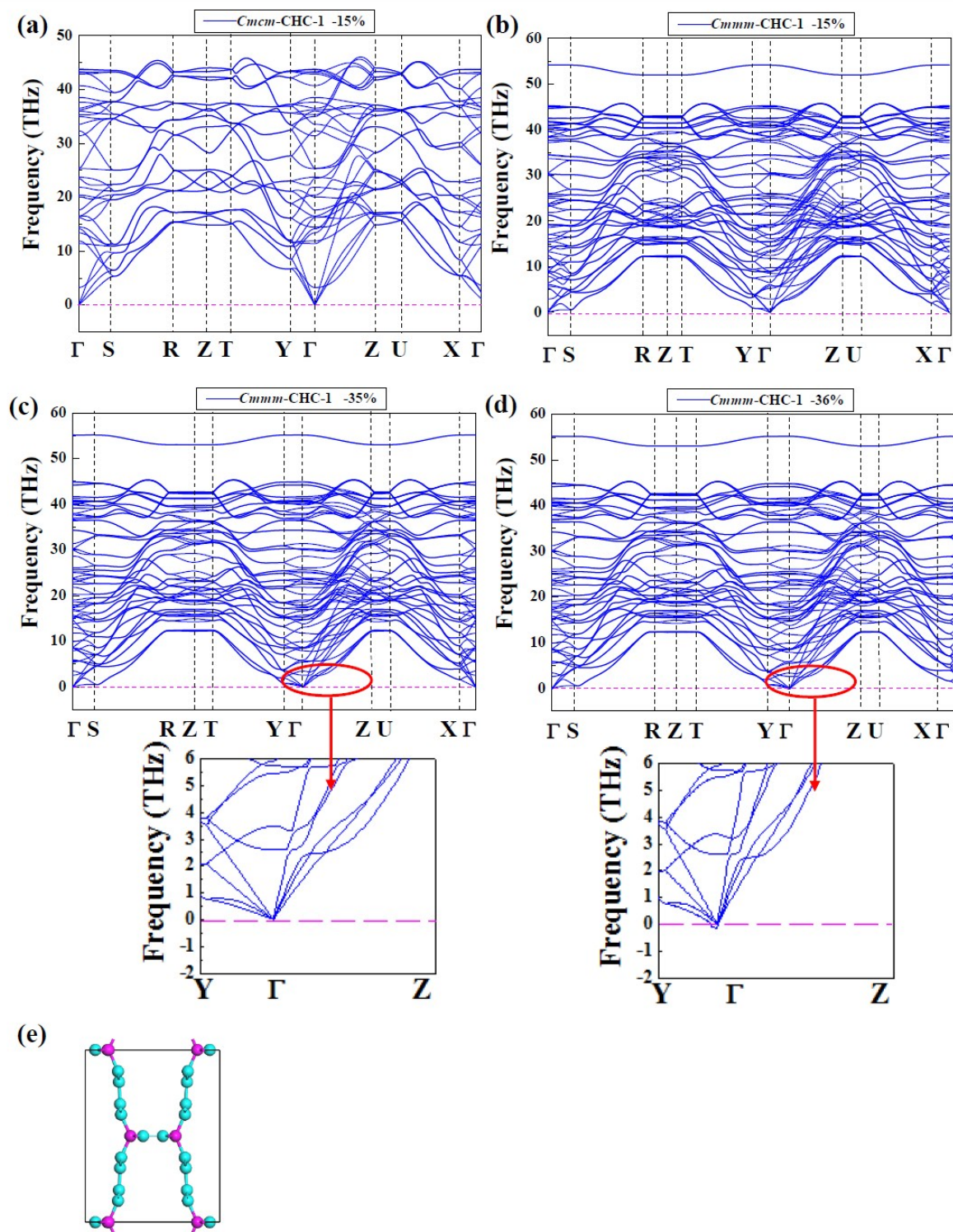


Figure S11. **The projected DOS.** (a) *Cmcm*-CHC-1 and (b) *Cmmm*-CHC-1 at the strain of -15% (compression) along the armchair direction.

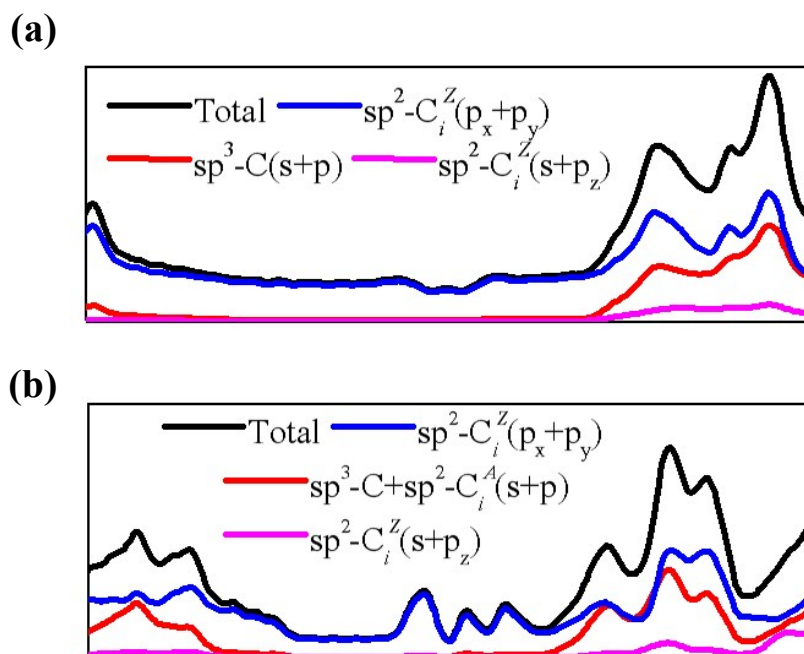
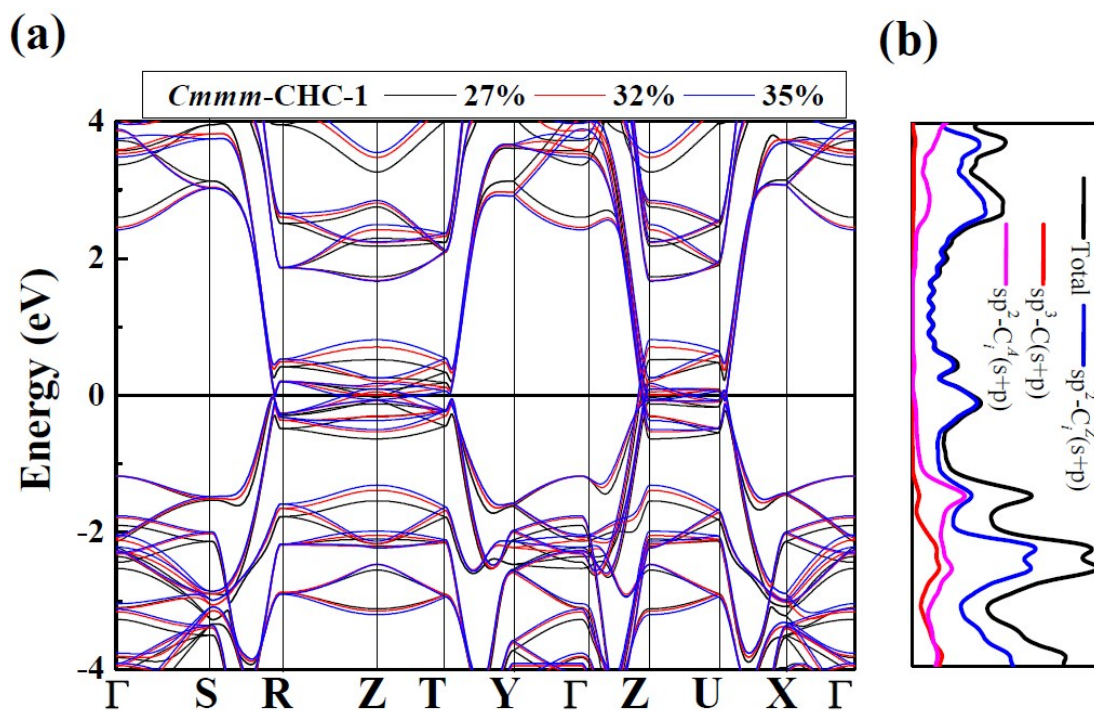


Figure S12. **The band structure** (a) of *Cmmm*-CHC-1 at the strain of -27%, -32%, and -35% (compression) along the armchair direction and the projected DOS (b) at the strain of -32%.



References

1. G. Kresse and J. Hafner, *Physical Review B*, 1993, 48, 13115-13118.
2. G. Kresse and J. Furthmüller, *Physical Review B*, 1996, 54, 11169-11186.
3. J. P. Perdew, K. Burke and M. Ernzerhof, *Physical Review Letters*, 1996, 77, 3865-3868.
4. A. Togo, F. Oba and I. Tanaka, *Physical Review B*, 2008, 78, 134106.
5. A. Togo and I. Tanaka, *Scripta Materialia*, 2015, 108, 1-5.
6. Y. Wang, J. Lv, L. Zhu and Y. Ma, *Physical Review B*, 2010, 82, 094116.
7. H. Sun, S. Mukherjee and C. V. Singh, *Physical Chemistry Chemical Physics*, 2016, 18, 26736-26742.
8. C. Zhong, Y. Chen, Y. Xie, S. A. Yang, M. L. Cohen and S. B. Zhang, *Nanoscale*, 2016, 8, 7232-7239.
9. K. E. Spear and J. P. Dismukes, *Synthetic diamond: emerging CVD science and technology*, John Wiley & Sons, 1994.